

PREDICTIVE ROCK MASS CLASSIFICATION PARAMETER MODELS FROM ROCK MATERIAL ENGINEERING TESTS

Ahmad Faiz Salmanfarsi, Haryati Awang*

Faculty of Civil Engineering Technology, Universiti Malaysia
Pahang Al-Sultan Abdullah, Lebuhraya Tun Razak, 26300
Kuantan, Pahang, Malaysia

Article history

Received

2 August 2024

Received in revised form

3 January 2025

Accepted

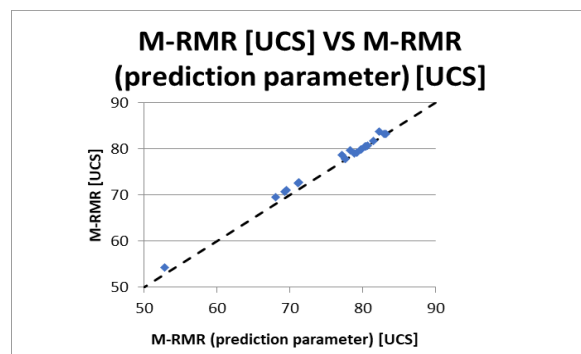
20 January 2025

Published Online

22 August 2025

*Corresponding author
haryatiawang@ump.edu.my

Graphical abstract



Abstract

Rock mass classification is one of the most widely used method for assessment of rock slope which is developed from empirical case studies. One of the most widely used are the Rock Mass Rating (RMR). Most of the rock mass classifications were developed through discrete rating of parameters, meaning that a high subjectivity from the practitioner is involved in assigned rating of the parameters. Thus, continuous functions were developed in order to reduce the subjectivity when assigning values to the parameters. This study attempts to develop predictive model of selected parameters from several available continuous function in the RMR rock mass classification, using input of laboratory test of engineering properties of weathered granite. Multiple regression analysis indicated several of the physical properties of weathered granite are statistically significant in predicting the parameters of strength of intact rock material and intact rock alterability. These prediction models are validated through graphical plotting of calculated continuous function RMR using measured field and laboratory test value for the parameter against calculated continuous function RMR using prediction model for parameter value. Several of the continuous function RMR show no statistical difference in mean value between the two values of continuous function RMR, indicating that calculation using prediction models for the parameter are closely similar to calculation using actual field and laboratory measurement of the parameter. Regression analysis are carried out for the rest of the continuous function RMR to provide correction factor to use these prediction models as parameters in the continuous function RMR.

Keywords: Rock engineering properties, granite, rock mass classification, rock mass rating, regression analysis

Abstrak

Klasifikasi jisim batu adalah salah satu kaedah yang paling banyak digunakan untuk penilaian cerun batuan, dan dibangunkan daripada kajian kes empirikal. Salah satu daripada klasifikasi jisim batuan adalah Rock Mass Rating, atau RMR. Kebanyakan klasifikasi jisim batuan dibangunkan menggunakan pemeringkatan diskret, atau discrete ranking, untuk parameter, di mana terdapat tahap subjektiviti yang tinggi dari pengguna klasifikasi jisim batuan ketika memberi penilaian untuk nilai untuk setiap parameter. Dari masa ke masa, beberapa fungsi berterusan, atau continuous function, telah dibangunkan untuk mengurangkan subjektiviti apabila memberikan nilai kepada parameter dalam pengelasan jisim batuan. Kajian ini dijalankan untuk

tujuan pembangunan model ramalan parameter daripada beberapa fungsi berterusan yang sedia ada dalam pengelasan jisim batuan RMR, menggunakan data daripada ujian makmal sifat kejuruteraan granit terluluhawa. Analisis regresi berperingkat, atau multiple regression analysis, telah menunjukkan beberapa sifat fizikal granit terluluhawa adalah signifikan secara statistik dalam meramal parameter kekuatan bahan batuan utuh. Atau strength of intact rock material, dan kebolehubahan batuan utuh, atau intact rock alterability. Model ramalan ini kemudiannya disahkan melalui pemplotan grafik, di mana nilai RMR fungsi berterusan menggunakan nilai parameter dari lapangan dan makmal dipetakan melawan nilai RMR fungsi berterusan menggunakan nilai parameter modal ramalan.. Beberapa RMR fungsi berterusan tidak menunjukkan perbezaan statistik dalam nilai purata antara dua nilai fungsi berterusan RMR, di mana pengiraan menggunakan model ramalan untuk parameter adalah hampir sama dengan pengiraan menggunakan nilai parameter yang diukur dari lapangan dan makmal. Analisis regresi dijalankan untuk fungsi berterusan RMR yang selebihnya, di mana factor pembetulan diberi untuk penggunaan model ramalan untuk parameter bagi fungsi berterusan RMR tersebut.

Kata kunci: Sifat kejuruteraan batuan, batuan granit, pengelasan jisim batuan, klasifikasi jisim batuan, analisa regresi

© 2025 Penerbit UTM Press. All rights reserved

1.0 INTRODUCTION

Slope failures are serious hazards that takes place all over the world, leading to damages to infrastructures and loss of lives. With the continuous development over low-lying areas, more and more constructions are carried out involving highland and steep rock slopes – leading to more potential of the risk of slope failures. Slope failures or landslides have been reported to be one of the most destructive natural disasters in Malaysia, right after flooding [1]. The effect of slope failures affect both the harming of lives, and the economic development, such as where highways are constructed along rock slopes [2,3]. Although case studies of local slope failures have indicated that design failure as one of the most significant contributing factor to the slope failing, the geological factors, or the underlying rock unit and geological structures, have been reported to be the main contributing factor to landslides globally [4,5]. Indeed, several local cases of slope failures that occur despite constant preventative measures taken have suggested that these are undertaken without properly considering the underlying rock unit and geological structures [6] which would suggest incorrect slope protection measures without proper understanding of the underlying rock unit and geological features of the slopes. This is because the rock mass that forms the slope is heterogenous and anisotropic, which consist of discontinuities that are produced from stresses due to tectonic activities or weathering effect [7] that may be potential trigger of slope failures.

Due to the concern of slope instability, several methods of evaluating the quality of rock slope and

its potential for failure have been developed over the years. Generally, the evaluation methods could be divided into kinematic analysis, limit equilibrium, numerical modelling, and empirical methods [8]. For assessment of rock slope, the kinematic analysis is a commonly used method for practitioner in Malaysia, where engineering assessment of rock slope is based on measurement and analysis of discontinuities by stereographic projection – or more specifically, the projection of the discontinuity orientation by pole, depicting the dip and dip direction of joint on 2D stereonet [9,10]. Recent case studies by Abdul Rahim *et al.* (2023) [11] have shown a preference for kinematic analysis for local rock slope assessment, followed with stability rating and numerical analysis.

The rock mass classification, which falls under the empirical method for rock modelling, is one of the more widely used method for local rock slope assessments. Initially the rock mass classifications are developed for underground excavation, where they are used for underground project design [12,13]. They are very useful for both engineers and geologist working on rock slopes, where they provide a common basis, and are simple and effective in representing rock mass quality and summing up relevant key practices [14,15]. The rating in rock mass classifications are developed from numerical value and weighting factors of several parameters, where an empirical formula were substituted from weighting values to obtain final rating for a rock mass [16]. By calibrating relevant parameters such as surface excavation, it made it possible to include various other functions in classifying cut slopes, such as the role of triggering factors of earthquake and water movement [17]. From the early development of rock

mass classification, it continues to be used by practitioners as the empirical method for assessing slope stability during design phase [8]. The simplicity and ability to manage uncertainty have made the rock mass classifications continue to be used over the years [18]. Comparative analysis among the different rock mass classifications by recent studies [8, 19-21] prove the validity of the method for assessment of rock slope.

Most of the rock mass classification ratings are created using discrete rating, which relies on the subjective experience of the user when assigning ranking to the parameters of the classification. To reduce some of the subjectivity when ranking the parameters of the rock mass classification, the discrete functions are converted into continuous functions, where exact values for each parameters are used to calculate a more objective ranking values. Examples of continuous rating of rock mass classifications are found in the works of Şen and Sadagah (2003), Rehman *et al.* (2018), and Kundu *et al.* (2020) [22,23,24]. The use of continuous function in rock mass classification calculation makes it possible to integrate predictive models of engineering values of rock materials with data from laboratory testing, calculated through correlation analysis.

To achieve the objective of the study of proposing predictive model for parameters of rock

mass classification, a portion of Karak-Lanchang and Sri Jaya-Gambang area of Pahang, Malaysia is selected as the study area. The general area belongs under the Central Belt of Peninsular Malaysia, where the geology is dominated by Carboniferous to Permian aged sedimentary and metasedimentary rocks, Triassic interbedded sedimentary rocks and volcanics, Jurassic continental sedimentary deposits, and granitic bodies, which are the Tembeling Group, Semantan Formation, and Seri Jaya Beds, as well as volcanic and granite rocks [25, 26].

Granitic rock slopes were selected, where the rock mass characteristic is studied. The selected study areas are shown in Figure 1. These granites are a part of the Eastern Belt Peninsular Malaysia granites, which are predominantly I-type, with reported age that spans from Permian to Triassic and Upper Cretaceous [27,28]. Recent studies of the granite in Pahang have noted on their role as the parent rock for bauxite, and as the concentration of rare earth minerals [29]. Selected slopes are ones which are structurally controlled – which refers to slopes that exhibit discontinuity sets which may potentially trigger potential rock failures [30]. No exhaustive rock mass classification of the granites in the area have been reported so far, which is the main focus of this study.

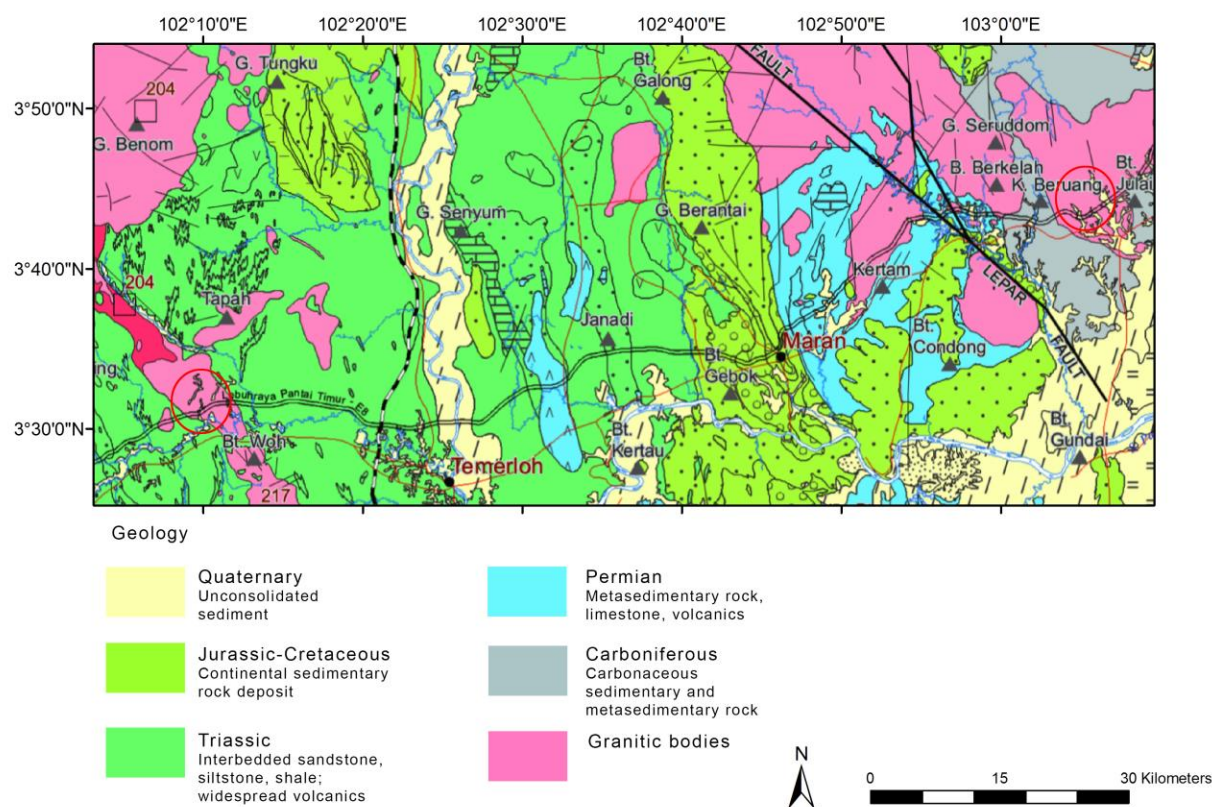


Figure 1 Geology of the study area. Red circles are areas where the slopes are studied in this study

2.0 METHODOLOGY

Initial field mapping were carried out using the scanline method. For each scanlines, the mapped parameters are the rock unit, weathering condition, and discontinuity sets. The rock types were identified visually, using reference charts for grain sizes, colour, and texture. Alongside identification of the rock units, the weathering profile of the slope is also noted, with mapping of the weathering using measurements from the Schmidt Rebound Hammer. For mapping of discontinuity, several parameters relevant to the classification of rock mass were measured: the type of discontinuity; the dip and dip direction; length or persistence; width or aperture; weathering; spacing; condition of joint surface; and presence of water. Finally, the slope geometry – height, dip, and dip direction – were measured. The mapping process of the geologic unit, weathering, and discontinuity follows the standard of the British Standards Institution (BSI) (2018) [31], BSI (2015) [32] and International Society for Rock Mechanics (ISRM) (2007) [33] respectively. The procedures for field mapping is shown in Figure 2.



(a) Discontinuity measurement of slope



(b) Weathering grade measurement of slope using Schmidt Rebound Hammer

Figure 2 Field mapping procedures for rock mass classifications

Five slope study areas were selected for this study, where several sets of discontinuity sets were mapped out for the calculation of rock mass classification. Each of the discontinuity sets have their own distinct parameters, where varying value of the rock mass classification can be calculated. The summary of the basic features of the slopes and discontinuity sets are shown in Table 1.

Selected samples of rock material of the varying weathering grade are collected for physical and strength tests in the laboratory. Physical tests covered are the specific gravity (SG), porosity (n), moisture content (MC), slake durability index (Id_2), and ultrasonic pulse velocity (UPV). Strength tests carried out for the samples are the laboratory Schmidt Rebound hammer, or surface hardness (R) tests, point load strength (PLS) tests, and uniaxial compressive strength (UCS) tests. The apparatus for laboratory tests are shown in Figure 3, and the summary of the standard used for the tests are shown in Table 2.

Table 1 Summary of study sites, with mapped discontinuity sets

| Site | Slope height | Slope dip/dip direction | Discontinuity sets | | | | | |
|--------|--------------|-------------------------|--------------------|----------|----------|----------|----------|----------|
| | | | J1 | J2 | J3 | J4 | J5 | J6 |
| Site 1 | 21 m | 70°/140° | 31°/051° | 78°/064° | 78°/092° | 79°/182° | 81°/222° | 72°/263° |
| Site 2 | 28 m | 70°/155° | 75°/033° | 34°/054° | 89°/074° | 78°/178° | 55°/275° | - |
| Site 3 | 18 m | 66°/330° | 73°/045° | 56°/135° | 71°/253° | - | - | - |
| Site 4 | 56 m | 70°/190° | 86°/253° | 79°/315° | 75°/359° | - | - | - |
| Site 5 | 17 m | 82°/024° | 88°/072° | 79°/184° | 12°/287° | 70°/325° | - | - |



(a) Apparatus for measurement of specific gravity, porosity, and moisture content



(b) Apparatus for measurement of slake durability index, Id₂



(c) Apparatus for measurement of ultrasonic pulse velocity, UPV



(d) Apparatus for measurement of point load strength, PLS



(e) Apparatus for measurement of uniaxial compressive strength, UCS



(f) Apparatus for measurement of laboratory Schmidt Rebound Hammer value, R

Figure 3 Laboratory procedures for measuring engineering properties of weathered granite

Table 2 Summary of tests carried out on weathered granite

| Tests | Sample type | Standards | Num of samples |
|-------------------------------|------------------------------------|------------------|----------------|
| Physical properties test | Aggregate samples and core samples | ISRM (2007) [33] | 87 |
| Ultrasonic velocity test | Core samples | ISRM (2015) [34] | 66 |
| Slake-durability test | Aggregate samples | ISRM (2007) [33] | 68 |
| Surface hardness | Core samples | ISRM (2015) [34] | 71 |
| Point load strength | Aggregate samples | ISRM (2007) [33] | 183 |
| Uniaxial compressive strength | Core samples | ISRM (2007) [33] | 66 |

Several rock mass classifications were used in this study. The parameters of each classification are as follows:

The original Rock Mass Rating (RMR), or RMR₈₉ developed by Bieniawski (1989) [14] was calculated using five parameters: strength of intact rock material (uniaxial compressive test (UCS) or point load strength (PLS)) (R_s); rock quality designation, or RQD (R_{RQD}); spacing between discontinuities (R_{SD}), condition of discontinuities (R_{CD}); and groundwater condition (R_{CG}). The equation of RMR₈₉ is shown in Eq. 1:

$$RMR_{89} = R_s + R_{RQD} + R_{SD} + R_{CD} + R_{CG} \quad (1)$$

The 2014 RMR update (RMR₁₄) by Celada et. al (2014) [35] combined both parameter of R_{RQD} and R_{SD} of RMR₈₉, to form the parameter of density of discontinuities (R_{DD}); the rating for R_{CD} parameter is modified (R_{CD14}); and a new parameter of intact rock alterability rating (R_{IRA}) was added, using the values from slake durability tests. The equation of RMR₁₄ is shown in Eq. 2.

$$RMR_{14} = R_s + R_{DD} + R_{CD14} + R_{IRA} + R_{CG} \quad (2)$$

The difference of the ranking of rating in the two RMR classifications is summarized in Table 3.

Table 3 Classification of the parameters across the different rock mass classifications of RMR

| Rock mass classification | RMR ₈₉ | RMR ₁₄ |
|--|--|--|
| Parameters | | |
| Strength of intact rock material (UCS, PLS, R) | R_s (0-15) | R_s (0-15) |
| Discontinuities (Orientation, spacing, RQD, discontinuity condition) | R_{RQD} (3-20) R_{SD} (5-20) R_{CD} (0-30) | R_{DD} (0-40) $R_{CD(REVISED)}$ (0-20) R_{CG} (0-15) |
| Groundwater (presence or flow rate) | R_{CG} (0-15) | R_{CG} (0-15) |
| Other parameters | - | R_{IRA} (0-10) |

Independent of the two RMR rating, the calculation of RMR ratings are also calculated through several continuous functions of the RMR. The different continuous functions of RMR used in this study is summarized in Table 4, where alternative

names are proposed to distinguish the different classifications for analysis purpose: M-RMR [UCS] and M-RMR [PLS] for the continuous function RMR of Şen and Sadagah (2003) [22] that uses UCS and PLS as the strength of intact rock material parameter respectively; M-RMR₈₉₋₁₈ and M-RMR₁₄₋₁₈ for the continuous function RMR of Rehman et al. (2018) [23] that uses UCS as the strength of intact rock material parameter for the original RMR₈₉ and RMR₁₄ respectively; M-RMR₈₉₋₂₀ [UCS], M-RMR₈₉₋₂₀ [PLS] and M-RMR₈₉₋₂₀ [R] for the continuous function RMR₈₉ of Kundu et al. (2020) [24] that uses UCS, PLS and R as the strength of intact rock material parameter respectively; and M-RMR₁₄₋₂₀ [UCS], M-RMR₁₄₋₂₀ [PLS] and M-RMR₁₄₋₂₀ [R] for the continuous function RMR₁₄ of Kundu et al. (2020) [24] that uses UCS, PLS and R as the strength of intact rock material parameter respectively.

Statistical analysis were used in prediction models to determine selected parameters of the continuous functions of the RMR, where multiple regression analysis are used to determine the most significant engineering properties of rock material in predicting the parameters. In this paper, the analysis predicts the parameters of the strength of intact rock material and intact rock alterability from measured physical properties of weathered granite. The prediction models of the parameters are then substituted into the continuous function RMR calculation, and are validated against measurement of continuous function RMR using actual field and laboratory measurement of the parameters. Validation tests were carried out through the graphical plotting of the identity line / 45° line and through paired sample t-test analysis.

3.0 RESULTS AND DISCUSSION

The results of the physical properties and strength properties of the weathered granite of the slopes are shown in Table 5 and Table 6 respectively, where weathering grade from Grade II to Grade V was observed. Comparison with other published engineering values of weathered granite shows the measured values falls under typically observed engineering properties of weathered granite [36, 37, 38, 39].

Table 4 Continuous function for RMR

| Parameters / Continuous function RMR | Şen and Sadagah (2003) [22] | Rehman et al. (2018) [23] | Kundu et al. (2020) (RMR89) [24] | Kundu et al. (2020) (RMR14) [24] |
|---|--------------------------------|---|--|--|
| Strength of intact rock: UCS (MPa) | $R_{UCS} = 0.075 UCS$ | $R_{UCS} = 0.126 UCS - 0.0004 UCS^2$ [UCS ≤ 110 MPa] $R_{UCS} = 0.475 UCS^{0.626}$ [UCS ≥ 110 MPa] | $R_{UCS} = 0.42 UCS - 0.01 ^{0.65} - 0.01$ If using R as input parameter, UCS = $9.97 e^{(0.02R_p)}$ | $R_{UCS} = 0.42 UCS - 0.01 ^{0.65} - 0.01$ If using R as input parameter, UCS = $9.97 e^{(0.02R_p)}$ |
| Strength of intact rock: PLS (MPa) | $R_{PLS} = 1.67 (1 + PLS)$ | - | $R_{PLS} = (28 / (1 + 10^{(0.02 - 0.15 PLS)})) - 13$ | $R_{PLS} = (28 / (1 + 10^{(0.02 - 0.15 PLS)})) - 13$ |
| RQD (%) | $R_{RQD} = 0.2 RQD$ | $R_{RQD} = 0.22 RQD - 0.0002 RQD^2$ | $R_{RQD} = 0.317 RQD - 0.07 ^{0.9} - 0.02$ | - |
| Discontinuity spacing (mm) | $R_{SD} = 24 + 151 \log (SP)$ | $R_{SD} = 2.281 \ln (SD) - 3.41$ [SD = 5–200 mm] $R_{SD} = 4.171 \ln (SD) - 13.51$ [SD = 200–900 mm] $R_{SD} = 6.250 \ln (SD) - 27.55$ [SD = 900–2000 mm] | $R_{SD} = 1.94 SD^{0.316} - 1.5$ | - |
| Discontinuity density | - | $R_{DD} = 34.442 e^{-0.046 DD}$ [DD ≤ 20] $R_{DD} = 22.8 - 0.457 DD$, [DD ≥ 20] | - | $R_{DD} = 42.35 - 7.4 DD^{0.443}$ |
| Groundwater condition (L/min) | $R_{CG} = 10 - 2.9 \log (GWI)$ | - | $R_{CG} = 165 / (GWI + 11)$ | $R_{CG} = 165 / (GWI + 11)$ |
| Discontinuity condition | - | - | $R_{CD89} = 1 / (0.166 + 0.05 DL)$ | $R_{CD14} = 5 - 0.5 DL$ |
| -Discontinuity length (m) | - | - | $R_{DA} = 1 / (0.166 + 0.25 DA)$ | - |
| -Discontinuity aperture (mm) | - | - | $89R_{DR} = 0.3 JRC$ | $14R_{DR} = 0.25 JRC$ |
| -Discontinuity roughness | - | - | $89R_{HI} = 6 - (4HI^4 / (256 + HI^4))$ | $14R_{HI} = 5 - (3 HI^2 / (10 + HI^2))$ |
| -Discontinuity infilling: hard infilling (mm) | - | - | $89R_{SI} = 162 / (27 + SI^3)$ | $14R_{SI} = 1 / (0.2 + 0.2 SI)$ |
| -Discontinuity infilling: soft infilling (mm) | - | - | $89R_{SW} = 6.3 / (1 + 10^{(0.032I5 - 1.3)})$ | $14R_{SW} = 5.3 / (1 + 10^{(0.03 I5 - 1.22)})$ |
| -Discontinuity surface weathering | - | - | - | $R_{RA} = (14.3 / (1 + 10^{(0.78 - 0.015 Id2)})) - 2$ |
| Intact rock alterability (%) | - | - | - | - |
| Name of RMR classification used in the analysis of this paper | M-RMR [UCS] M-RMR [PLS] | M-RMR ₈₉₋₁₄ M-RMR ₁₄₋₁₈ | M-RMR ₈₉₋₂₀ [UCS] M-RMR ₈₉₋₂₀ [PLS] M-RMR ₈₉₋₂₀ [R] | M-RMR ₁₄₋₂₀ [UCS] M-RMR ₁₄₋₂₀ [PLS] M-RMR ₁₄₋₂₀ [R] |

UCS = Uniaxial Compressive Strength; PLS = Point Load Strength Index; R = Schmidt Rebound Hammer value; ρ = rock's specific gravity/density; RQD = Rock Quality Designation; SD = Spacing of Discontinuities; GWI = Ground Water Inflow per 10 m tunnel length; DL = Discontinuity Length; DA = Discontinuity Aperture; JRC = Joint Roughness Coefficient; HI = thickness of Hard Infilling; SI = thickness of Soft Infilling; SW = Surface Weathering; I5 = weathering in percentage; Id2 = Slake durability Index

Table 5 Summary of physical properties of granite

| Properties | WG | Avg | Min | Max | Std dev | Skewness |
|-------------------------|-----|-------|-------|-------|---------|----------|
| SG (g/cm ³) | II | 2.57 | 2.47 | 2.63 | 0.04 | -ve |
| | III | 2.47 | 2.30 | 2.60 | 0.08 | -ve |
| | IV | 2.29 | 2.03 | 2.42 | 0.13 | -ve |
| | V | 2.03 | 1.70 | 2.29 | 0.26 | -ve |
| n (%) | II | 2.17 | 0.80 | 5.90 | 1.17 | +ve |
| | III | 6.13 | 1.65 | 12.10 | 3.04 | +ve |
| | IV | 12.91 | 8.06 | 20.75 | 4.47 | +ve |
| | V | 25.40 | 14.79 | 34.73 | 7.51 | +ve |
| MC (%) | II | 0.85 | 0.31 | 2.39 | 0.48 | +ve |
| | III | 2.52 | 0.64 | 5.17 | 1.34 | +ve |
| | IV | 5.77 | 3.33 | 10.23 | 2.38 | +ve |
| | V | 13.04 | 6.49 | 20.47 | 5.44 | +ve |
| Id ₂ (%) | II | 98.78 | 97.08 | 99.85 | 0.66 | -ve |
| | III | 94.58 | 91.29 | 97.11 | 2.00 | -ve |
| | IV | 80.08 | 63.74 | 89.10 | 8.08 | -ve |

| Properties | WG | Avg | Min | Max | Std dev | Skewness |
|------------|-----|---------|---------|---------|---------|----------|
| | V | 13.34 | 13.34 | 13.34 | - | - |
| UPV (m/s) | II | 4756.76 | 3568.73 | 5567.01 | 536.97 | -ve |
| | III | 3841.99 | 2658.19 | 4794.37 | 735.49 | -ve |
| | IV | 1196.01 | 511.35 | 1713.96 | 507.71 | -ve |

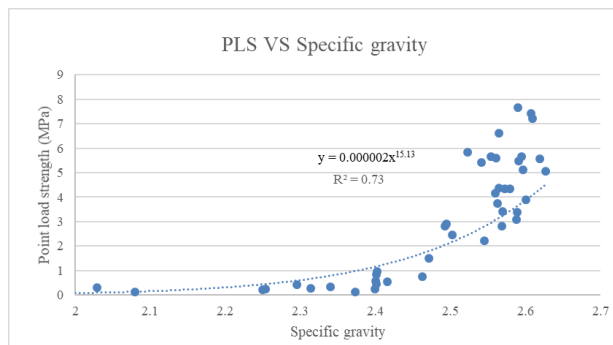
WG = weathering grade; SG = specific gravity; n = porosity; MC = moisture content; Id_2 = Slake durability index; UPV = ultrasonic pulse velocity

Table 6 Summary of strength properties of granite

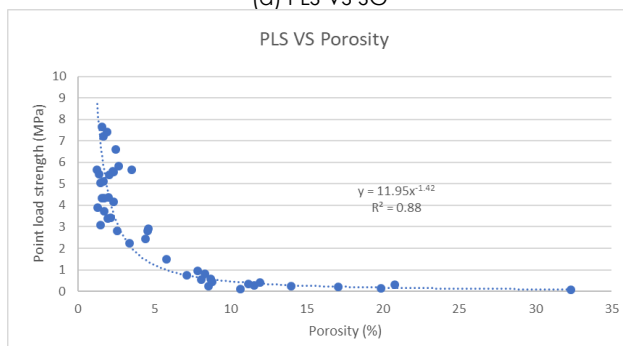
| Properties | WG | Avg | Min | Max | Std dev | Skewness |
|------------|-----|-------|-------|--------|---------|----------|
| R | II | 52.9 | 38 | 65.5 | 8.2 | +ve |
| | III | 40.0 | 27.8 | 47.7 | 5.5 | -ve |
| | IV | 19.4 | 14 | 26.6 | 5.3 | +ve |
| PLS (MPa) | II | 4.87 | 1.56 | 11.36 | 2.08 | +ve |
| | III | 1.17 | 0.33 | 2.45 | 0.68 | +ve |
| | IV | 0.30 | 0.057 | 0.70 | 0.20 | +ve |
| | V | 0.06 | 0.06 | 0.06 | - | - |
| UCS (MPa) | II | 87.63 | 60.65 | 119.53 | 12.80 | -ve |
| | III | 69.96 | 41.95 | 88.84 | 14.80 | +ve |
| | IV | 11.32 | 5.56 | 17.99 | 6.26 | +ve |

WG = weathering grade; R = Schmidt Rebound Hammer value; PLS = point load strength; UCS = uniaxial compressive strength

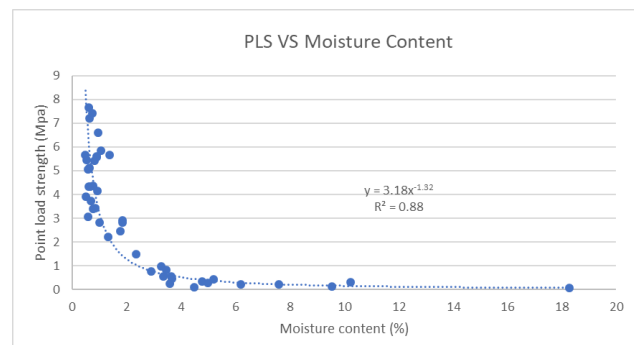
The relationship between PLS and physical properties of weathered granite is shown in Figure 4.



(a) PLS VS SG



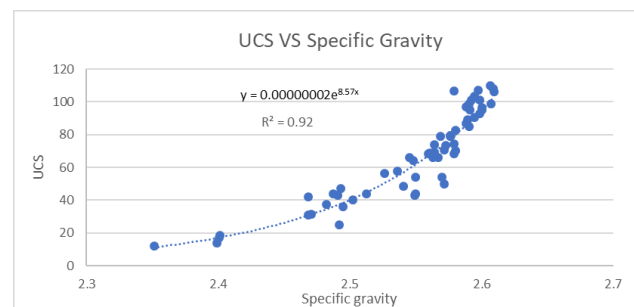
(b) PLS VS n



(c) PLS VS MC

Figure 4 Relationship between PLS and physical properties of weathered granite

The relationship between UCS and physical properties of weathered granite is shown in Figure 5.



(a) UCS VS SG

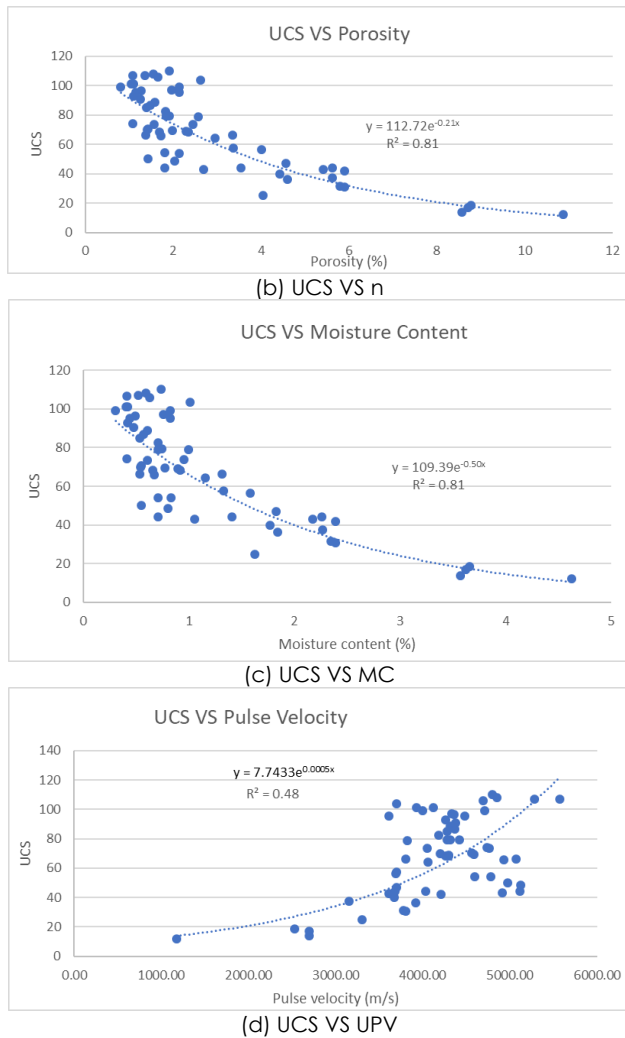
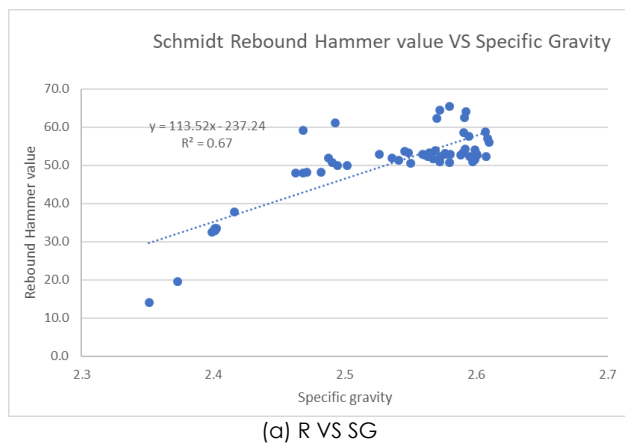


Figure 5 Relationship between UCS and physical properties of weathered granite

The relationship between R and physical properties of weathered granite is shown in Figure 6.



(a) R VS SG

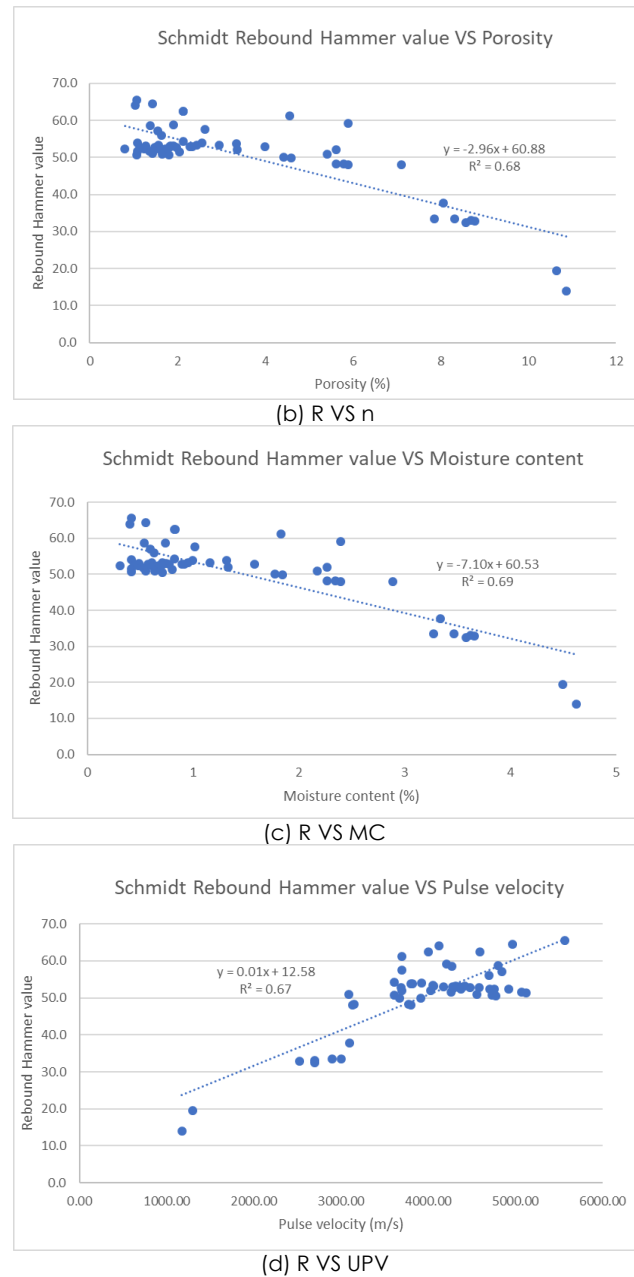


Figure 6 Relationship between R and physical properties of weathered granite

The relationship between Id_2 and physical properties of weathered granite is shown in Figure 7.

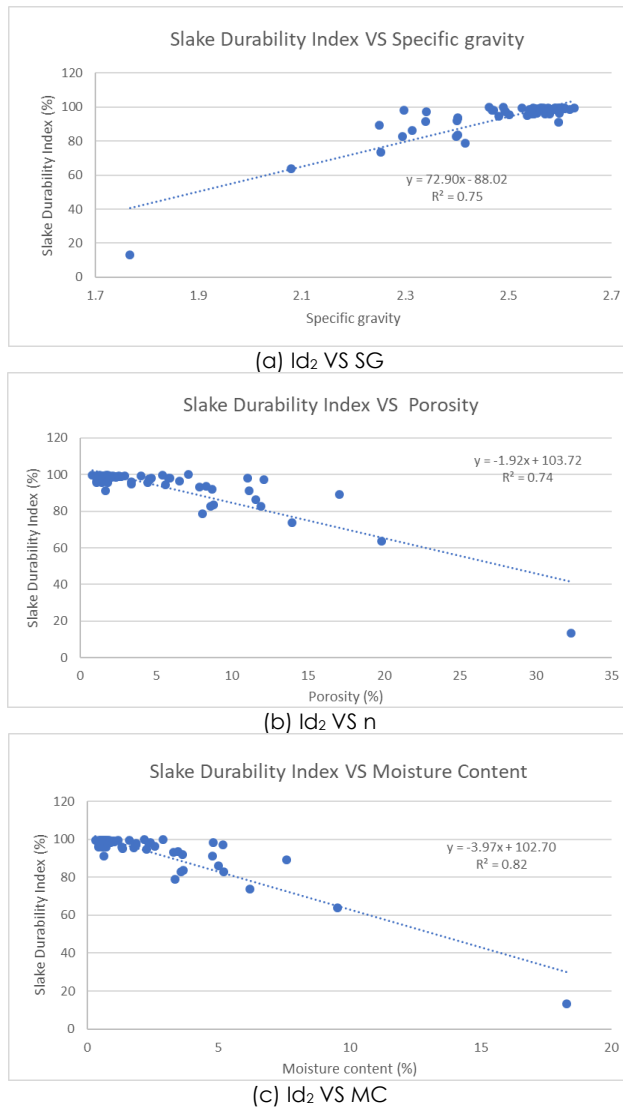


Figure 7 Relationship between Id₂ and physical properties of weathered granite

Multiple regression analysis between the strength of intact rock material and (PLS, UCS, R) and intact rock alterability (Id₂) is carried out, with the results summarized in Table 7. It is noted that most of the parameters exhibit very low p-value, with most ranging in the value of 0.000.

Table 7 Summary of multiple regression analysis of engineering parameters VS physical properties of weathered granite

| Parameters | Coefficient of Determination (R ²) | p-value |
|------------|--|---------|
| PLS VS SG | 0.735 | 0.250 |
| PLS VS n | | 0.000 |
| PLS VS MC | | 0.000 |
| UCS VS SG | 0.919 | 0.000 |
| UCS VS n | | 0.001 |
| UCS VS MC | | 0.000 |
| UCS VS UPV | | 0.526 |
| R VS SG | 0.866 | 0.186 |
| R VS n | | 0.000 |

| Parameters | Coefficient of Determination (R ²) | p-value |
|-----------------------|--|---------|
| R VS MC | | 0.000 |
| R VS UPV | | 0.006 |
| Id ₂ VS SG | 0.903 | 0.112 |
| Id ₂ VS n | | 0.000 |
| Id ₂ VS MC | | 0.000 |

PLS = point load strength; UCS = uniaxial compressive strength; R = Schmidt Rebound Hammer value; Id₂ = Slake durability index; SG = specific gravity; n = porosity; MC = moisture content; UPV = ultrasonic pulse velocity

A second multiple regression analysis is carried out, where only statistically significant parameters are considered in the regression. The cutoff point used to determine statistically significant parameter are parameters with p-value that are equal or lower than 0.005 ($p \leq 0.05$). The results of the multiple regression analysis are summarized in Table 8.

Table 8 Summary of multiple regression analysis of engineering parameters VS physical properties of weathered granite, using statistically significant parameters from result of first multiple regression analysis

| Parameters | Coefficient of Determination (R ²) | p-value |
|-----------------------|--|---------|
| PLS VS n | 0.726 | 0.000 |
| PLS VS MC | | 0.000 |
| UCS VS SG | 0.919 | 0.000 |
| UCS VS n | | 0.001 |
| UCS VS MC | | 0.000 |
| R VS n | 0.861 | 0.000 |
| R VS MC | | 0.000 |
| R VS UPV | | 0.006 |
| Id ₂ VS n | 0.900 | 0.000 |
| Id ₂ VS MC | | 0.000 |

PLS = point load strength; UCS = uniaxial compressive strength; R = Schmidt Rebound Hammer value; Id₂ = Slake durability index; n = porosity; MC = moisture content; SG = specific gravity; UPV = ultrasonic pulse velocity

With the second regression analysis, all the parameters exhibit very low p-value, indicating that the engineering properties are statistically significant in explaining the relationship with the predicted parameter of strength of intact rock material and intact rock alterability. From the multiple regression, prediction model can be proposed from the value of predictor coefficient for each input parameter and constant value, as well as the calculation of the model's Coefficient of Determination (R²). Equation for the predicted models for parameters of strength of intact rock material and intact rock alterability from physical properties of weathered granite are summarized in Table 9.

Table 9 Summary of model equations for predicting strength of intact rock material and intact rock alterability from physical properties of granite

| Predicted parameters | Equation | R ² |
|----------------------|--|----------------|
| PLS | PLS = 5.81 - 1.252n + 2.42 MC | 0.726 |
| UCS | UCS = -2498.059 + 993.159 SG - 56.680 n + 172.082 MC | 0.919 |
| R | R = 37.306 + 54.478 n - 134.135 MC + 0.003 UPV | 0.861 |
| Id ₂ | Id ₂ = 99.16 + 4.47 n - 12.63 MC | 0.900 |

PLS = point load strength; UCS = uniaxial compressive strength; R = Schmidt Rebound Hammer value; Id₂ = Slake durability index; n = porosity; MC = moisture content; SG = specific gravity; UPV = ultrasonic pulse velocity

From the developed prediction models for RMR parameter from engineering properties, the predicted parameters were then used in selected continuous functions of RMR, which are then validated through the means of plotting of calculated value on the identity line, and statistical test through paired sample t-test. In the plotting of the continuous function RMR value on the identity line, the y-axis represents calculated continuous function RMR using actual parameters reading from field and laboratory tests, while the x-axis represents calculated continuous function RMR using the parameters calculated from the prediction models.

The plot on the identity line is given in Figure 8 – Figure 17. The plot showed that for calculation of different continuous function of RMR, there is varying level of data scattering around the identity line, with some data closely clustered to the line – indicating that the relationship between the two measured continuous function RMR approach that of a 1:1 relationship – whereas others show plotting of data that are more scattered, indicating that there are possible significant deviation or differences between the two measured continuous function RMR.

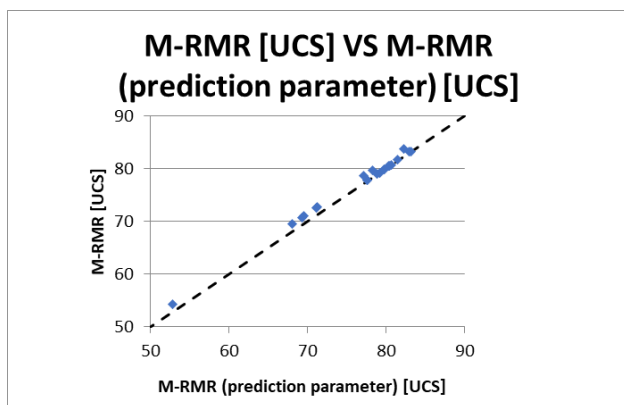


Figure 8 Identity line plot between M-RMR and M-RMR (prediction parameter), using prediction parameter UCS as input

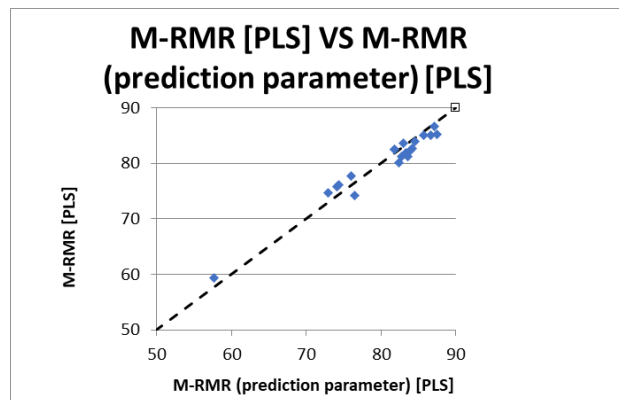


Figure 9 Identity line plot between M-RMR and M-RMR (prediction parameter), using prediction parameter PLS as input

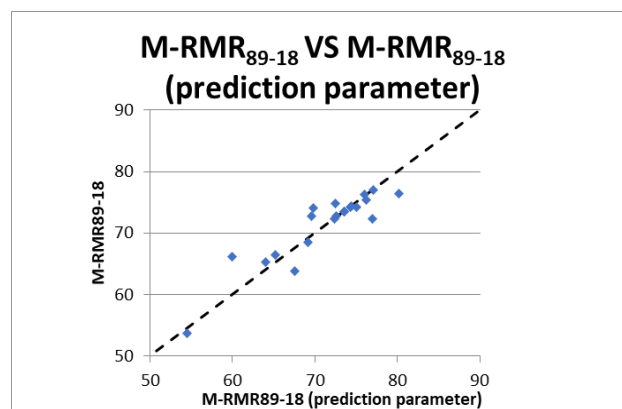


Figure 10 Identity line plot between M-RMR₈₉₋₁₈ and M-RMR₈₉₋₁₈ (prediction parameter), using prediction parameter UCS as input

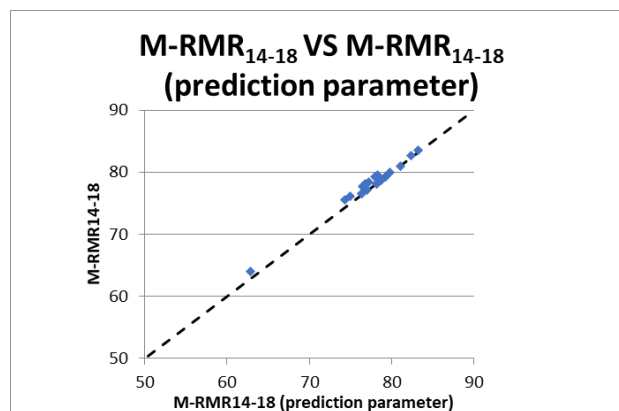


Figure 11 Identity line plot between M-RMR₁₄₋₁₈ and M-RMR₁₄₋₁₈ (prediction parameter), using prediction parameter UCS as input

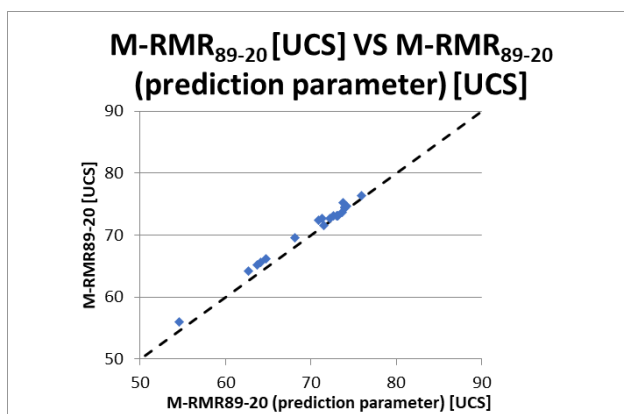


Figure 12 Identity line plot between M-RMR₈₉₋₂₀ and M-RMR₈₉₋₂₀ (prediction parameter), using prediction parameter UCS as input

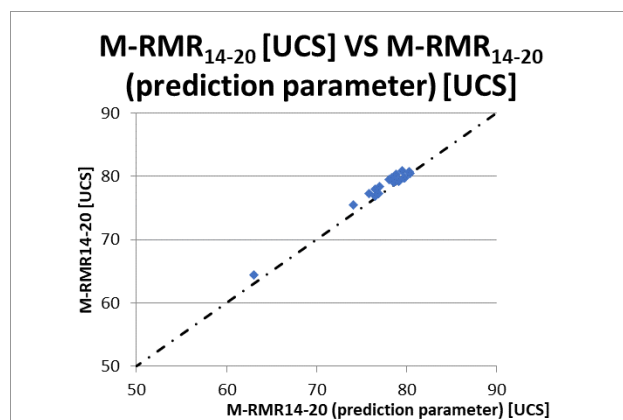


Figure 15 Identity line plot between M-RMR₁₄₋₂₀ and M-RMR₁₄₋₂₀ (prediction parameter), using prediction parameter UCS as input

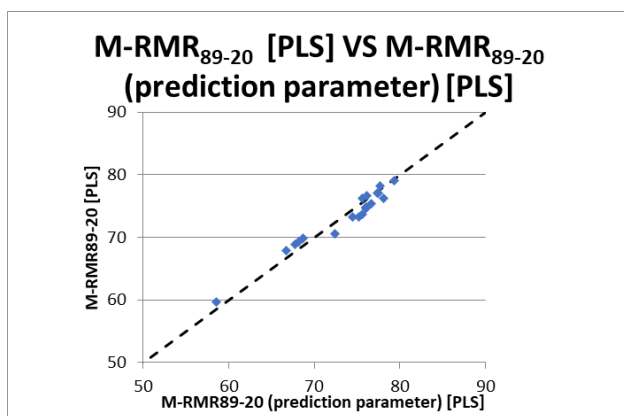


Figure 13 Identity line plot between M-RMR₈₉₋₂₀ and M-RMR₈₉₋₂₀ (prediction parameter), using prediction parameter PLS as input

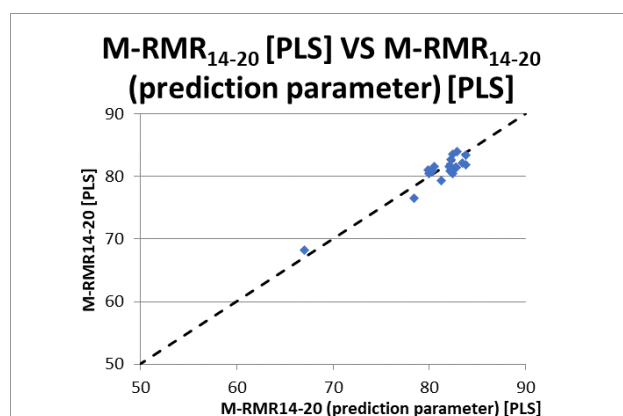


Figure 16 Identity line plot between M-RMR₁₄₋₂₀ and M-RMR₁₄₋₂₀ (prediction parameter), using prediction parameter PLS as input

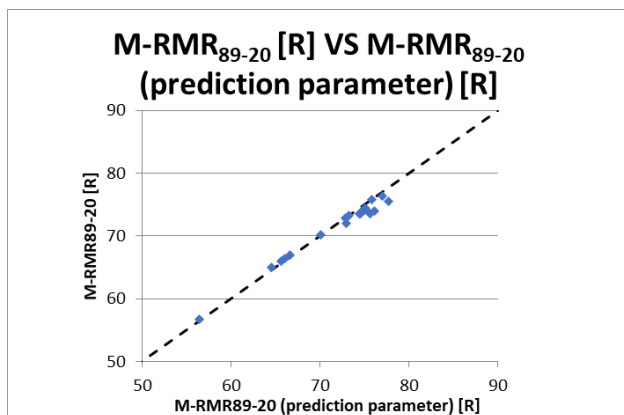


Figure 14 Identity line plot between M-RMR₈₉₋₂₀ and M-RMR₈₉₋₂₀ (prediction parameter), using prediction parameter R as input

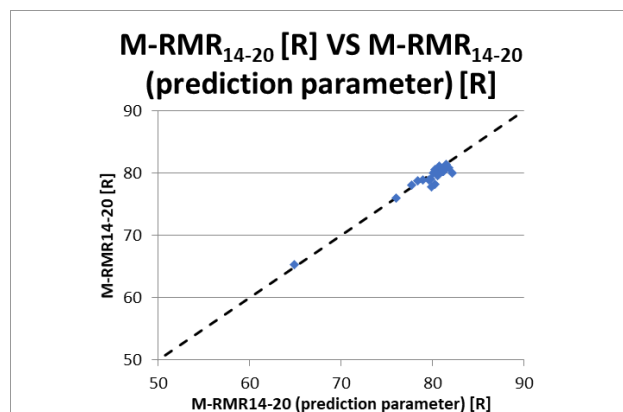


Figure 17 Identity line plot between M-RMR₁₄₋₂₀ and M-RMR₁₄₋₂₀ (prediction parameter), using prediction parameter R as input

In order to further validate the relationship between the two measured continuous function RMR, analysis were carried out using t-test between paired means. A summary of the t-test is shown in Table 10. Result from the paired means t-test would indicate that the two average readings of measured continuous functions would be statistically significant if the p-value falls below the cutoff point ($p \leq 0.05$) and t-statistic value that exceeds the amount of calculated t-critical value. From the analysis, it was found that the calculated continuous function RMR of M-RMR [PLS], M-RMR₈₉₋₁₈, M-RMR₈₉₋₂₀ [PLS], and M-RMR₁₄₋₂₀ [PLS] exhibit no significant difference between the means of the calculated continuous function RMR using input parameter from actual field and laboratory test and the means of the calculated continuous function RMR using prediction models of parameters.

Table 10 Summary of t-test of paired means between calculated continuous function RMR using actual parameter input and calculated continuous function RMR using prediction parameter input

| Continuous function RMR | t-Stat | P(T<=t) two-tail | t Critical two-tail |
|------------------------------|--------|------------------|---------------------|
| M-RMR [UCS] | 4.85 | 0.00 | 2.09 |
| M-RMR [PLS] | -1.33 | 0.20 | 2.09 |
| M-RMR ₈₉₋₁₈ | 0.24 | 0.81 | 2.09 |
| M-RMR ₁₄₋₁₈ | 4.30 | 0.00 | 2.09 |
| M-RMR ₈₉₋₂₀ [UCS] | 5.63 | 0.00 | 2.09 |
| M-RMR ₈₉₋₂₀ [PLS] | -1.76 | 0.09 | 2.09 |
| M-RMR ₈₉₋₂₀ [R] | -3.44 | 0.00 | 2.09 |
| M-RMR ₁₄₋₂₀ [UCS] | 5.63 | 0.00 | 2.09 |
| M-RMR ₁₄₋₂₀ [PLS] | -1.76 | 0.09 | 2.09 |
| M-RMR ₁₄₋₂₀ [R] | -3.44 | 0.00 | 2.09 |

Due to the other continuous function RMR indicating that there are significant differences between the means of the calculated continuous function RMR using input parameter from actual field and laboratory test and the means of the calculated continuous function RMR using prediction models of parameters, regression analysis were carried out in order to apply correction factor to use the calculated continuous function RMR using prediction models of parameters, where coefficient and intercept of the regression equation are applied in order to achieve values that are close to the calculated continuous function RMR using input parameter from actual field and laboratory test. The summary of the regression analysis is shown in Table 11. Results from the p-value of the F-statistic indicate that the regression analysis were significant in contributing to the model ($p \leq 0.05$) and that the calculated continuous function RMR using prediction models of parameters is significant positive predictor of the calculated continuous function RMR using input parameter from actual field and laboratory test ($p \leq 0.05$).

An overall Summary of the overall prediction models of continuous function of RMR using physical properties of rock materials as prediction parameter is summarized in Table 12.

Table 11 Summary of statistical analysis of regression analysis between calculated continuous function RMR and calculated continuous function RMR using prediction parameter input

| Continuous function RMR name | Prediction parameter input | F-stat | F-stat p-value | R ² | t-test | P-value | Correction equation |
|------------------------------|-----------------------------|---------|----------------|----------------|--------|---------|---|
| M-RMR [UCS] | UCS | 3057.05 | 0.00 | 0.99 | 55.29 | 0.00 | M-RMR [UCS] = 0.94M-RMR [predicted UCS] + 5.50 |
| M-RMR ₁₄₋₁₈ | UCS | 977.36 | 0.00 | 0.98 | 31.26 | 0.00 | M-RMR ₁₄₋₁₈ = 0.92M-RMR ₁₄₋₁₈ [predicted UCS] + 6.38 |
| M-RMR ₈₉₋₂₀ [UCS] | UCS | 402.09 | 0.00 | 0.99 | 45.04 | 0.00 | M-RMR ₈₉₋₂₀ [UCS] = 0.92M-RMR ₈₉₋₂₀ [predicted UCS] + 6.30 |
| M-RMR ₈₉₋₂₀ [PLS] | UCS from R | 1321.02 | 0.00 | 0.99 | 36.35 | 0.00 | M-RMR ₈₉₋₂₀ [R] = 0.89M-RMR ₈₉₋₂₀ [predicted UCS from R] + 7.37 |
| M-RMR ₈₉₋₂₀ [R] | UCS, Id ₂ | 147.72 | 0.00 | 0.89 | 26.73 | 0.00 | M-RMR ₁₄₋₂₀ [UCS] = 0.92M-RMR ₁₄₋₂₀ [predicted UCS] + 6.99 |
| M-RMR ₁₄₋₂₀ [UCS] | UCS from R, Id ₂ | 373.96 | 0.00 | 0.95 | 19.34 | 0.00 | M-RMR ₁₄₋₂₀ [R] = 0.91M-RMR ₁₄₋₂₀ [predicted UCS from R] + 6.88 |
| M-RMR ₁₄₋₂₀ [R] | UCS | 3057.05 | 0.00 | 0.99 | 55.29 | 0.00 | M-RMR [UCS] = 0.94M-RMR [predicted UCS] + 5.50 |

UCS = Uniaxial compressive strength; PLS = Point load strength; R = Schmidt Rebound Hammer value; Id₂ = Slake durability index

Table 12 Summary of prediction models of rock mass classification parameters and corrected predicted model for calculating continuous function RMR using the prediction rock mass classification parameter

| Prediction model for input parameters | R ² | Continuous function RMR tested | Reference for continuous function RMR | Correction equation | R ² |
|---|----------------|--------------------------------|---------------------------------------|---|----------------|
| UCS = -2498.06 + 993.16SG - 56.68n + 172.08MC | 0.92 | M-RMR [UCS] | Şen and Sadagah (2003) [22] | M-RMR [UCS] = 0.94M-RMR [predicted UCS] + 5.50 | 0.99 |
| PLS = 5.81 - 1.25n + 2.42MC | 0.73 | M-RMR [PLS] | Şen and Sadagah (2003) [22] | - | - |
| UCS = -2498.06 + 993.16SG - 56.68n + 172.08MC | 0.92 | M-RMR ₈₉₋₁₈ | Rehman <i>et al.</i> (2018) [23] | - | - |
| UCS = -2498.06 + 993.16SG - 56.68n + 172.08MC | 0.92 | M-RMR ₁₄₋₁₈ | Rehman <i>et al.</i> (2018) [23] | M-RMR ₁₄₋₁₈ = 0.92M-RMR ₁₄₋₁₈ [predicted UCS] + 6.38 | 0.98 |
| UCS = -2498.06 + 993.16SG - 56.68n + 172.08MC | 0.92 | M-RMR ₈₉₋₂₀ [UCS] | Kundu <i>et al.</i> (2020) [24] | M-RMR ₈₉₋₂₀ [UCS] = 0.92M-RMR ₈₉₋₂₀ [predicted UCS] + 6.30 | 0.99 |
| PLS = 5.81 - 1.252n + 2.42MC | 0.73 | M-RMR ₈₉₋₂₀ [PLS] | Kundu <i>et al.</i> (2020) [24] | - | - |
| R = 37.31 + 54.48n - 134.14MC + 0.003UPV | 0.86 | M-RMR ₈₉₋₂₀ [R] | Kundu <i>et al.</i> (2020) [24] | M-RMR ₈₉₋₂₀ [R] = 0.89M-RMR ₈₉₋₂₀ [predicted UCS from R] + 7.37 | 0.99 |
| UCS = -2498.06 + 993.16SG - 56.68n + 172.08MC | 0.92 | M-RMR ₁₄₋₂₀ [UCS] | Kundu <i>et al.</i> (2020) [24] | M-RMR ₁₄₋₂₀ [UCS] = 0.92M-RMR ₁₄₋₂₀ [predicted UCS] + 6.99 | 0.89 |
| Id ₂ = 99.16 + 4.47n - 12.63MC | 0.90 | | | | |
| PLS = 5.81 - 1.252n + 2.42MC | 0.73 | M-RMR ₁₄₋₂₀ [PLS] | Kundu <i>et al.</i> (2020) [24] | - | - |
| Id ₂ = 99.16 + 4.47n - 12.63MC | 0.90 | | | | |
| R = 37.31 + 54.48n - 134.14MC + 0.003UPV | 0.86 | M-RMR ₁₄₋₂₀ [R] | Kundu <i>et al.</i> (2020) [24] | M-RMR ₁₄₋₂₀ [R] = 0.91M-RMR ₁₄₋₂₀ [predicted UCS from R] + 6.88 | 0.95 |
| Id ₂ = 99.16 + 4.47n - 12.63MC | 0.90 | | | | |

UCS = Uniaxial compressive strength; PLS = Point load strength; R = Schmidt Rebound Hammer value; SG = specific gravity; n = porosity; MC = moisture content; UPV = ultrasonic pulse velocity; Id₂ = Slake durability index

4.0 CONCLUSION

In this study, several predicted parameters of rock mass classification parameters have been established. Relationship between physical properties of weathered granite – which are specific gravity, porosity, moisture content, and pulse velocity – were correlated with PLS, UCS, R, and Id₂ values. The predicted models of these engineering values are then used in several continuous function of RMR. Correlation analysis on predicted continuous function of RMR using input values of physical properties of weathered granite show high degree of predicting the value of calculated continuous function of RMR using input values of laboratory result for strength of intact rock material (PLS, UCS, R) and intact rock alterability (Id₂). Graphical plot of identity line and paired t-tests for means between calculated continuous function RMR using actual parameter and continuous function RMR using prediction parameter have identified relationship which show no statistically difference between the average readings of the two RMR values. Linear regression are used for the rest of continuous function RMR which showed statistically significant difference between the average readings of the two RMR values, where correction factors are proposed to explain the difference between the calculated continuous function using actual parameter and calculated continuous function using prediction parameter.

Acknowledgement

The authors would like to acknowledge the research support provided by Universiti Malaysia Pahang under the Geran Universiti Malaysia Pahang, grant number RDU190345, and the Postgraduate Research Grant Scheme, grant number PGRS2003207.

Conflicts of Interest

The authors declare that there is no conflict of interest regarding the publication of this paper.

References

- [1] Akter, A., Parvez, A., Rasheduzzaman, M., Hasan, M. M. & Islam, M. 2022. A Review on Landslide Susceptibility Mapping in Malaysia: Recent Trend and Approaches. *Asian Journal of Social Sciences and Legal Studies*. 4(5): 199–208. Doi: 10.34104/ajssl.022.01990208.
- [2] Awang, H., Salmanfarsi, A. F., Zaini, M. S. I., Mohamad Yazid, M. A. F. & Ali, M. I. 2021. Investigation of Groundwater Table Under Rock Slope by Using Electrical Resistivity Imaging at Sri Jaya, Pahang, Malaysia. IOP Conference Series: Earth and Environmental Science. 682: 012017. Doi: 10.1088/1755-1315/682/1/012017.
- [3] Zaini, M. S. I., Hasan, M., & Zolkepli, M. F. 2022. Urban Landfills Investigation for Leachate Assessment Using Electrical Resistivity Imaging in Johor, Malaysia. *Environmental Challenges*. 6: 100415.

- [4] Public Work Department. 2009. National Slope Master Plan Sectoral Report Research and Development. Kuala Lumpur: Jabatan Kerja Raya Malaysia.
- [5] Davies, T., Rosser, N. & Shroder, J. F. 2021. Landslide Hazards, Risks, and Disasters. Elsevier, Amsterdam. 674. Doi: 10.1016/C2018-0-02502-5.
- [6] Salmanfarsi, A. F., Awang, H. & Ali, M. I. 2020. Rock Mass Classification for Rock Slope Stability Assessment in Malaysia: A Review. *IOP Conference Series: Material Science and Engineering*. 712: 012035. Doi: 10.1088/1757-899X/712/1/012035.
- [7] Nagendran, S. K., Mohamad Ismail, M. A. & Wen, Y. T. 2019. 2D And 3D Rock Slope Stability Assessment Using Limit Equilibrium Method Incorporating Photogrammetry Technique. *Bulletin of the Geological Society of Malaysia*, 68: 133–139. Doi: 10.7186/bgsm67201913.
- [8] Zerradi, Y., Souissi, M., Soufi, A., Bennouna, R., Bahi, A. & Zaki, I. 2023. Slope Stability Assessment Using Slope Mass Rating (SMR), Key Block Theory, and Kinematic Analysis: A Case Study. *Journal of Southwest Jiaotong University*. 58(4). Doi: 10.35741/issn.0258-2724.58.4.45.
- [9] Tan, B. K. 2017. Engineering Geology in Malaysia – Some Case Studies. *Bulletin of the Geological Society of Malaysia*. 64: 65–79. Doi: 10.7186/bgsm64201707.
- [10] Moses, D., Shimada, H., Sasaoka, T., Hamanaka, A., Dintwe, T. K. & Wahyudi, S. 2020. Rock Slope Stability Analysis by Using Integrated Approach. *World Journal of Engineering and Technology*. 8: 405–428. Doi: 10.4236/wjet.2020.83031.
- [11] Abdul Rahim, A. F., Md Rafek, A. G., Serasa, A. S., Jaapar, A. R., Goh, T. L., Roslee, R., Lee, K. E., Nguyen, X. H. & Tran, V. X. 2023. A Review of Rock Slope Stability Assessment Practice in Malaysia. *Sains Malaysiana*. 52(2): 399–416.
- [12] Bieniawski, Z. T. 1993. Classification of Rock Masses for Engineering: The RMR System and Future Trends. In Hudson, J. A. (Ed). *Comprehensive Rock Engineering*, Vol. 3: Rock Testing and Site Characterization - Principles, Practice & Projects. Pergamon Press, New York. 553–573.
- [13] Hussin, H. & Arifin, M. H. 2023. Rock Mass Classification for Rock Mass in Tunnelling and Underground Excavation - Development, Limitation and Way Forward. *Bulletin of the Geological Society of Malaysia*. 75: 13–23. Doi: 10.7186/bgsm75202303.
- [14] Bieniawski, Z. T. 1989. *Engineering Rock Mass Classifications: A Complete Manual for Engineers and Geologists in Mining, Civil, and Petroleum Engineering*. John Wiley & Sons, New York. 250.
- [15] Singh, B. & Goel, R. K. 2012. *Engineering Rock Mass Classification*. Butterworth-Heinemann, Oxford. 365. Doi: 10.1016/C2010-0-64994-7.
- [16] Rusydy, I., Ismet Canbulat, I., Zhang, C., Wei, C. & McQuillan, A. 2024. The Development and Implementation of Design Flowchart For Probabilistic Rock Slope Stability Assessments: A Review. *Geoenvironmental Disasters*. 11(28): 1–26. Doi: 10.1186/s40677-024-00290-9.
- [17] Pantelidis, L. 2009. Rock Slope Stability Assessment through Rock Mass Classification Systems. *International Journal of Rock Mechanics and Mining Sciences*. 46(2): 315–325. Doi: 10.1016/j.ijrmms.2008.06.003.
- [18] Erharter, G. H., Bar, N., Hansen, T. F., Jain, S. & Marcher, T. 2024. International Distribution and Development of Rock Mass Classification: A Review. *Rock Mechanics and Rock Engineering*. 2024. Doi: 10.1007/s00603-024-04215-8.
- [19] Sardana, S., Verma, A. K., Singh, A. & Laldinpuia. 2019. Comparative Analysis of Rockmass Characterization Techniques for the Stability Prediction of Road Cut Slopes along NH-44A, Mizoram, India. *Bulletin of Engineering Geology and the Environment*. 78(8): 5977–5989.
- [20] Khanna, R. & Dubey, R. K. 2021. Comparative Assessment of Slope Stability along Road-cuts through Rock Slope Classification Systems in Kullu Himalayas, Himachal Pradesh, India. *Bulletin of Engineering Geology and the Environment*. 80: 993–1017. Doi: 10.1007/s10064-020-02021-4.
- [21] Alejano, L. R. 2024. Rock Mass Classification Systems: A Useful Rock Mechanics Tool, Often Misused. *Rock Mechanics and Rock Engineering*. 2024. Doi: 10.1007/s00603-024-04087-y.
- [22] Şen, Z. & Sadagah, B. H. 2003. Modified Rock Mass Classification System by Continuous Rating. *Engineering Geology*. 67(3–4): 269–280. Doi: 10.1016/S0013-7952(02)00185-0.
- [23] Rehman, H., Ali, W., Naji, A. M., Kim, J. & Yoo, H. K. 2018. Empirical Evaluation of Rock Mass Rating and Tunneling Quality Index System for Tunnel Support Design. *Applied Sciences*. 8: 782. Doi: 10.3390/app8050782.
- [24] Kundu, J., Sarkar, K., Singh, A. K. & Singh, T. N. 2020. Continuous Functions and a Computer Application for Rock Mass Rating. *International Journal of Rock Mechanics and Mining Sciences*. 129: 104280. Doi: 10.1016/j.ijrmms.2020.104280.
- [25] Simon, N., Mat Akhir, J., Napiah, A. & Tan, H. K. 2008. Development of Landslide Database along km 160 – km 190, East Coast Highway, Pahang. *Warta Geologi*. 34(5&6): 233–238.
- [26] Tan, H. K., Mat Akhir, J., Napiah, A. & Simon, N. 2008. Pemetaan Ramalan Potensi Tanah Runtuh di Sepanjang km160-190 Lebuhraya Pantai Timur dengan Pendekatan Sistem Maklumat Geografi: Kaedah Statistik. *Warta Geologi*. 34(5&6): 239–242.
- [27] Yu, Y., Xin Qian, X., Mustapha, K. A., Sheldrick, T. C., Gan, C., Zhang, Y. & Wang, Y. 2022. Late Paleozoic–Early Mesozoic Granitic Rocks in Eastern Peninsular Malaysia: New Insights for the Subduction and Evolution of the Paleo-Tethys. *Journal of Asian Earth Sciences*. 239: 105427. Doi: 10.1016/j.jseaes.2022.105427.
- [28] Nugraheni, R. D., Sunjaya, D. & Agustini, S. 2018. Regional Tectonic and Geochemical Approach to Distinguish Bauxite Characteristics in Pahang, Malaysia and West Kalimantan, Indonesia. *IOP Conference Series: Earth and Environmental Science*. 212: 012026. Doi: 10.1088/1755-1315/212/1/012026.
- [29] Ghani, A. A., Shahjamal, M., Ng, T. F., Ismail, N. E. H., Mohamad Zulkifley, M. T., Islami, N. ... Masor, A. F. 2019. Ce Anomaly in I-Type Granitic Soil from Kuantan, Peninsular Malaysia: Retention of Zircon in the Weathering Product. *Sains Malaysiana*. 48(2): 309–315. Doi: 10.17576/jsm-2019-4802-06.
- [30] Awang, H., Salmanfarsi, A. F., Misbahuddi, A. Z. & Ali, M. I. 2021. Slope Stability Analysis of Rock Mass using Rock Mass Rating and Slope Mass Rating. *IOP Conference Series: Earth and Environmental Science*. 682: 012015. Doi: 10.1088/1755-1315/682/1/012015.
- [31] British Standards Institution. 2018. *Geotechnical Investigation and Testing. Identification, Description and Classification of Rock. Part 1: Identification and Description*. BS EN ISO 14689:2018. London: BSI.
- [32] British Standards Institution. 2015. *Code of Practice for Site Investigations*. BS 5930: 2015+A1:2020. London: BSI.
- [33] Ulusay, R. & Hudson, J. A. 2007. *The Complete ISRM Suggested Methods for Rock Characterization, Testing and Monitoring: 1974-2006*. Ankara: International Society of Rock Mechanics Commission on Testing Methods, 2007.
- [34] Ulusay, R. 2015. *The ISRM Suggested Methods for Rock Characterization, Testing and Monitoring: 2007-2014*. Switzerland: Springer International Publishing.
- [35] Celada, B., Tardáguila, I., Varona, P., Rodríguez, A. & Bieniawski, Z.T. 2014. Innovating Tunnel Design by an Improved Experience-based RMR System. A. Negro, M. O. Cecilio Jr. & W. Bilfinger (Eds.). *Proceedings of the World Tunnel Congress* (pp. 1–9).
- [36] Mohamad, E. T., Latifi, N., Arefnia, A. & Isa, M. F. 2016. Effects of Moisture Content on the Strength of Tropicallly Weathered Granite from Malaysia. *Bulletin of Engineering Geology and the Environment*. 75: 369–390. Doi: 10.1007/s10064-015-0749-2.

- [37] Wengang, Z., Liang, H., Zixu, Z. & Yanmei, Z. 2021. Digitalization of Mechanical and Physical Properties of Singapore Bukit Timah Granite Rocks based on Borehole Data from Four Sites. *Underground Space*. 6(5): 483–491. Doi: 10.1016/j.undsp.2020.02.003.
- [38] Raj, J. K. 2023. Physical Characterization of the Weathering Profile over a Sheared, Biotite-muscovite Granite in Peninsular Malaysia. *Bulletin of the Geological Society of Malaysia*. 75, 25–36. Doi: 10.7186/bgsm75202304.
- [39] Suparmanto, E. K., Mohamad, E. T., Rathinasamy, V., Ahmad Legiman, M. K., Zainal, Z., Zainuddin, N. E. ... Armaghani, D. J. 2024. A Series of Regression Models to Predict the Weathering Index of Tropical Granite Rock Mass. *Environmental Earth Sciences*. 83(518): 2024. Doi: 10.1007/s12665-024-11742-8.